Surfaces and Interfaces 48 (2024) 104299

Contents lists available at ScienceDirect

Surfaces and Interfaces

journal homepage: www.sciencedirect.com/journal/surfaces-and-interfaces

Enhancing bonding of fresh concrete to steel through Laser Surface Texturing

Marida Pontrandolfi [a,b], Caterina Gaudiuso [b,*], Francesco Paolo Mezzapesa [b], Annalisa Volpe [a,b], Myriam Bevillon [c], Antonio Ancona [a,b]

[a] Intercollegiate Department of Physics "M. Merlin", University of Bari and Polytechnic University of Bari, Via G. Amendola 173, 70125 Bari, Italy
[b] National Research Council (CNR), Institute for Photonics and Nanotechnologies (IFN), Via G. Amendola 173, 70125 Bari, Italy
[c] Gunnebo Innovation Hub, Department of Physics "M. Merlin", Via G. Amendola 173, 70125 Bari, Italy

ARTICLE INFO

Keywords:
Concrete
Laser surface texturing
LIPSS
Mechanical interlocking
Adhesion

ABSTRACT

In this work, we investigated the adhesion between surface-treated stainless-steel samples and a standard cement mixture. Laser surface treatments such as Direct Laser Writing (DLW) and Laser-Induced Periodic Surface Structures (LIPSS) were employed, which resulted effective to reach up to 16-fold increase of adhesion compared to the untextured. A comparison with mechanical surface treatments, i.e., sandblasting, revealed that, although an increase of adhesion was achieved probably ascribable to the higher surface roughness, such improvement in terms of bonding strength was significantly lower than the one obtained with the laser surface texturing.

1. Introduction

Concrete is a composite material characterized by a continuous phase (or matrix), which is made by the mix of cement and water, and a discontinuous phase, which is mainly composed by aggregates, i.e., gravel and sand. The construction of urban infrastructures, bridges, dams, safety-related nuclear structures [1], and safes vaults and panels are only few of many examples in which this material is employed. Furthermore, the addition of reinforcements, i.e. polymers [2], metals [3], natural materials [4], steel rebars [5], and glasses or steel fibers [6, 7] marked a turning point in the growth of the concrete strength, and consequently of the products performances.

Nevertheless, when additional reinforcements are implemented to the concrete mixture to increase its strength, the adhesion between all the elements is crucial; in fact, the stronger the adhesion, the more stresses can be withstood by the structure, preserving it from cracks propagation that may lead to structural failure [8].

One way to improve the adhesion is to modify the concrete mixture recipe by adding other components such as latex [9], silica fume and methylcellulose [10]. But taking this approach can lead to a noticeable change of the concrete mechanical properties. An alternative strategy consists of treating the surface of the target where the concrete will adhere. In fact, while several mechanisms can be enlisted as underlying the adhesion between steel and concrete, e.g., electrochemical bonding, capillary suction, and mechanical anchoring, the last two are strongly related to the presence of defects on the steel surface where the fresh concrete is poured and can be influenced by a modification of the surface morphology. Capillary suction, i.e., the capability of transport of liquids through the pores of a porous medium acting as capillaries, leads to a very strong bonding in the case of smooth and impermeable surfaces such as metals and polymers [11]. Moreover, mechanical anchoring occurring through the asperities of the metal surface acting as traps for concrete and cement particles is the typical adhesion mechanism of concrete to a solid surface; this mechanism is commonly called mechanical interlocking [12]. In this case, the higher the number of interlocking sites, i.e., deviations from the ideally flat surface, the higher is the bond strength between the steel surface and the hardened concrete.

Once the contact between the concrete and a metallic surface is established, an interfacial transition zone (ITZ) is formed, which is a boundary layer that arises due to residual water spreading over the metal surface. This ITZ consists of three main phases [12]: the first 10–100 μm thick layer from the metal substrate is mainly composed of fine cement particles and water. The intermediate 5 mm is the mortar layer, made up of larger sand and cement grains. The last layer (~30 mm) is the actual concrete bulk, made up of the biggest gravel, sand and cement particles. According to the mechanical anchoring mechanism, for the concrete to adhere to the steel, the fresh mixture should penetrate

* Corresponding author.
E-mail address: caterina.gaudiuso@cnr.it (C. Gaudiuso).

https://doi.org/10.1016/j.surfin.2024.104299
Received 16 January 2024; Received in revised form 20 March 2024; Accepted 4 April 2024
Available online 15 April 2024

the irregularities of the steel surface. Therefore, in order to improve the mechanical anchoring, it is possible to suitably design a surface texturing pattern characterized by surface traps big enough to entrap more than one particle (typical size ranging from 1 to 100 μm). Moreover, a high density of such traps should be ensured, to increase the efficiency of the particle "entrapment" process.

To create an effective interlocking surface, a simple approach involves enhancing the roughness of the surface by using abrasive techniques like sandblasting. According to Hou et al., a significant improvement (~17%) in the bond strength between reinforcing bars and concrete can be obtained through sandblasting of reinforcing bars [13].

In the last few years, significant emphasis and endeavor is focused on altering the surface topography of material substrates via laser surface patterning. Laser Surface Texturing (LST) is an environmentally friendly and innovating surface modification process due to its ability to modify surface properties without affecting the bulk properties of the material. In fact, it is a single-step, non-contact, and fast surface processing which does not require any chemicals, masks, or expensive vacuum-based systems, so it is an ideal technique for working ideally any kind of materials [14,15]. Direct Laser Writing (DLW) on metals exploits a laser beam for precisely removing material from a solid substrate to create micro-scaled textures. One of the key advantages of this process is its ability to create precise features with high resolution and accuracy, making it a valuable tool for researchers and manufacturers who need to create any complex texturing designs with high precision. Another potentially effective laser texturing technique relies on the formation of the so-called Laser-Induced Periodic Surface Structures (LIPSS), i.e. highly regular, periodic nanostructures. Both of them offer unique advantages but some limitations: DLW allows at optimizing the mechanical anchoring through the ablation of tailored texture geometrical features (dimensions and depth) so that they meet the dimensions of each specific cement used in the concrete recipe. Unfortunately, this could result is a slower process compared to LIPSS generation, which however is not effective on the interlocking mechanism mentioned before, because of the low depth characterizing the nanoscale structures (around 200 nm). Nonetheless, LIPSS are able to confer a super-hydrophilic behavior to the as treated surfaces which can strongly strengthen the capillary suction mechanism of adhesion.

Both techniques are capable of altering the wettability of the treated surface [16,17] and revealed to be suitable in improving the bonding with coatings and adhesives. In [18,19,20] their application for increasing the bonding of adhesives to different laser treated substrates was reported. Moreover, the influence of the orientation of the texture with respect to the applied load was also reported. In [21] who worked on aluminum, it was clearly shown that producing on aluminum surface a texture perpendicular to the applied load direction resulted in a significant enhancement of the mechanical interlocking and then of the final adhesion of an epoxy resin. However, the exploitation of laser surface texture technique for enhancing the adhesion of cement mixtures to steel is still poorly investigated.

The first demonstration of the effectiveness of laser texturing in enhancing the adhesion of concrete to steel was reported by Makarova et al. that performed laser nanostructuring of a steel rebar in three different applied fluence regimes, i.e., near threshold, fluence equal to 1.5 times the ablation threshold, and fluence equal to 3 times the ablation threshold. They found that only the samples fabricated with the highest fluence, where nanospikes were generated, were able to improve improved adhesion with concrete [22]. However, no exhaustive investigations on the relationship between the laser induced surface texture topography and the strength of the bonding with the hardened concrete was performed.

This work fits in this framework and aims at investigating the adhesion between a treated stainless-steel surface and a cement mixture. Various surface laser treatments were applied, including LIPSS and Direct Laser Writing.

In the latter case, among all the different patterns and texture arrangements capable of enhancing the bonding strength of adhesives, i.e., dimples, directional grooves, crossed grooves [18], two different texturing designs were analyzed, i.e., longitudinal, and transversal micro-milled channels, to investigate the influence of the texture directionality, in analogy to [21].

To test the performances of the surface treatments in terms of adhesion, a standard pull-out test was custom designed taking as a model the experimental setup presented in [23]. A comparison with sandblasting treatment at different exposure times was also provided.

2. Materials and methods

2.1. Surface treatment methodologies

A Yb:KGW laser system from Light Conversion (Pharos PH1-SP-1.5 mJ, Vilnius, Lithuania) was employed to texture the steel samples. The beam was characterized by a wavelength of 1030 nm, a linear polarization, a diffraction-limited gaussian profile (M^2 ~1.25), a maximum average power of 6 W and a variable repetition rate, from single pulse up to 1 MHz. The laser beam exiting the source went through a half-wave waveplate followed by a polarizer, for the fine control of the laser power. The beam was then directed into a galvoscanner (IntelliScan 14 from ScanLab GmbH, Puchheim, Germany), equipped with an F-Theta focal lens with a focal length of 100 mm (LINOS F-Theta-Ronar 100 mm telecentric, Qioptiq Photonics GmbH), which controlled the scanning path of the focused beam on the target surface. The steel sample was held in an XYZ translation stage, and the scanning parameters and texture design were set using a software by SCANLAB (laserDESK).

To produce the sandblasted samples, polymeric sand was propelled over the surfaces using a portable sandblaster. Its nozzle was fixed at 20 cm from the samples for each exposure time (20 s and 2 min).

2.2. Materials and sample design

In this study, 3 mm-thick AISI304 stainless-steel sheets and a cement mixture composed by pozzolanic cement from Cementeria Costantinopoli S.r.l (EN 197–1 CEM IV/B-P 32,5 R, Barile, Italy) and coarse sand were used. Each steel sample was placed inside a customized 20mm-deep PLA 3D printed container, where then the cement mixture was poured, as schematically showed in Fig. 1(a); this was essential to ensure the contact between the cement mixture and the steel surface. The geometrical characteristics of the metal sample and the cement mixture recipe (cement/sand and water/cement ratios) are shown in Fig. 1(b).

A statistical evaluation of the final adhesion of the treated samples, as compared to the untreated one, was carried out by producing four samples for each texturing condition, i.e., sandblasting, LIPSS, longitudinal DLW channel, and transversal DLW channel, for averaging the results and determining the maximum error. In all cases, the treated area was 20×20 mm^2, much larger than the typical scale of the ITZ thickness (between 20 μm and 120 μm) to allow drawing general reliable data. As for sandblasting, two different treatment times were explored, i.e., 20 s and 2 min, to highlight the effect of the roughness. In fact, it is well known that the longer the exposure time, the higher the roughness of the surface [24]. The DLW samples were engraved with 80 μm-deep rectangular channels ablated on the sample surface. Thus, a regular repetition of micro-walls was textured, both longitudinally and transversally, at a distance equal to the width of the channel. A schematic of these textures is shown in Fig. 2, with their design parameters listed in Table 1.

The choice of their geometrical features, i.e., width and depth, aimed at influencing the mechanical anchoring, by generating substrate features able to entrap cement particles, whose dimensions in standard cement range from 1 to 100 μm [12]. However, thanks to the flexibility of laser technology, any shape can be potentially fabricated. The two different arrangements of the micro-structures were chosen in order to investigate their response with respect to the pulling direction. Indeed,

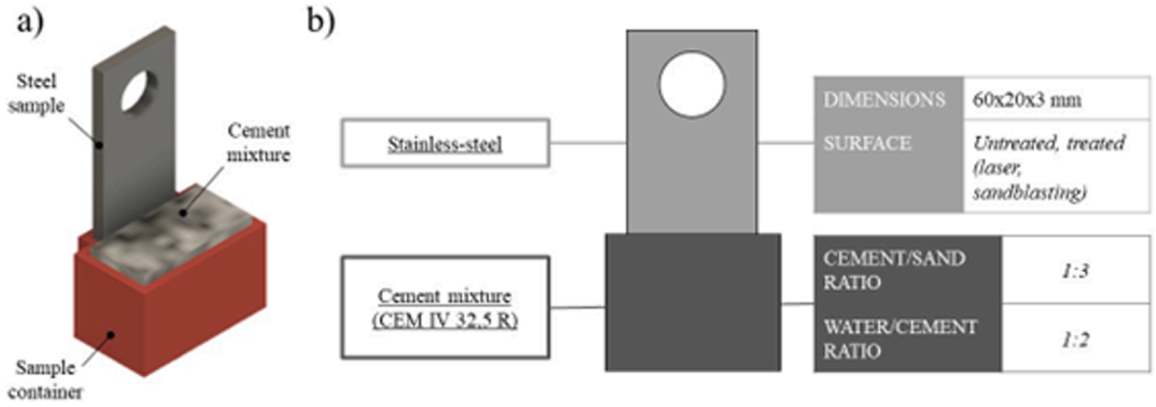

Fig. 1. Graphical representation of the sample: (a) assembled sample inside the 3D printed container; (b) sample specifications, underlining the dimensions, the surface treatments made on the steel sample and the cement mixture recipe. In order to optimize the adhesion testing procedure, a 10 mm diameter hole was drilled over the sample.

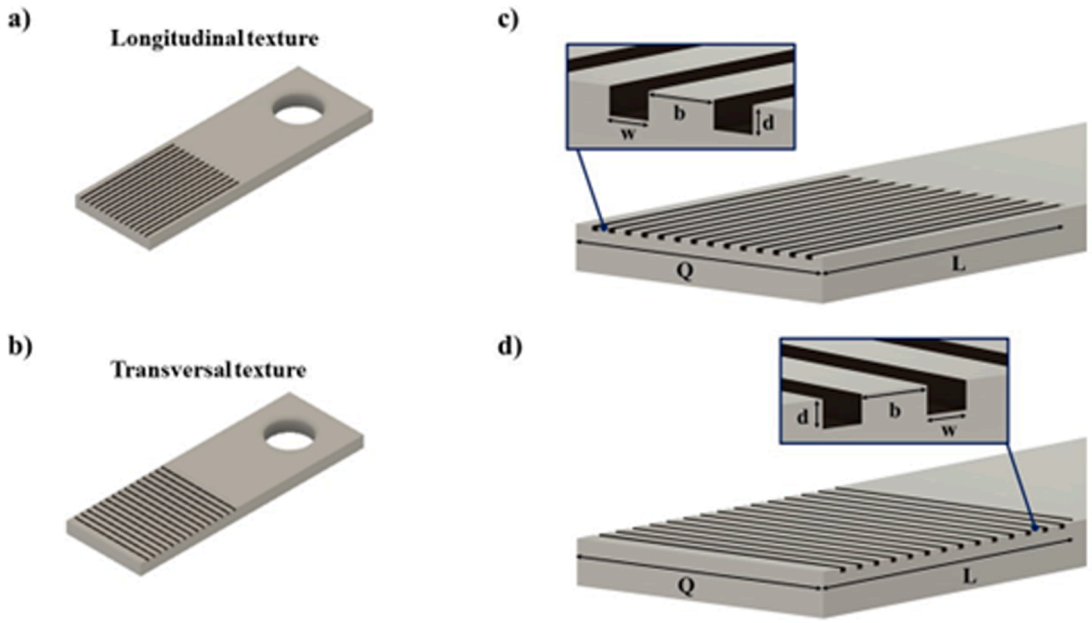

Fig. 2. Schematic representation on the sample with (a) longitudinal texture and (b) transversal texture. A more detailed representation of laser texturing in (c) longitudinal configuration and (d) transversal configuration is presented. In (c,d) L represents the length of the treated area (20 mm), Q the width of the treated area (20 mm), b the wall width (1 mm), w the channel width (500 μm), and d the channel depth (80 μm).

Table 1
Geometrical parameters taken into account for texturing design. The side labels are referring to Fig. 2.

Parameter	Side label	Value
Length of the treated area (mm)	L	20
Width of the treated area (mm)	Q	20
Wall width (mm)	b	1
Channel width (μm)	w	500
Channel depth (μm)	d	80

in the longitudinal texture, the channels and walls were parallel to the direction of the pull-out (Fig. 2a), while in the transversal texture, i.e., 90-degree rotated texture (Fig. 2b), the arrangement of the laser ablated micro-structures was orthogonal to the pull-out direction.

After the laser treatment, the samples were cleaned through sonication in 2-propanol for ten minutes to remove any ablation debris redeposited on their surface. Afterwards, the samples were inserted into the 3D printed containers (see Fig. 1a) and fresh cement mixture was immediately poured inside, ensuring the contact between the treated surface and the mixture. Adhesion tests were performed thirty days after the preparation of the samples, to guarantee the right curing time of the concrete. A scheme of the whole procedure is presented in Fig. 3.

2.3. Sample characterization

2.3.1. Morphological and chemical characterization

After the surface treatments, optical microscopy (Eclipse ME600; Nikon, Japan) was exploited to measure the depth of the engraved channels, while the measurement of the surface roughness was performed by optical profilometry (ContourGT InMotion; Bruker, USA). Furthermore, a Field Emission Scanning Electron Microscope (SEM) (Sigma; Zeiss, Germany) was employed to characterize the morphology of the LIPSS and analyze, by using Energy Diffraction X-ray spectroscopy (EDX), the chemical composition of the surface in order to evaluate if some cement sticked onto the steel samples after the pull-out tests.

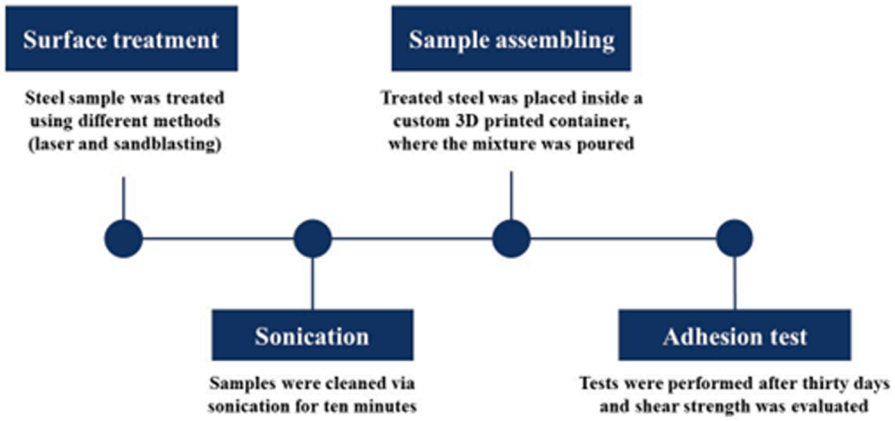

Fig. 3. Schematical view of the sample preparation procedures.

2.3.2. Adhesion evaluation procedure

To measure the adhesion strength between the steel and cement, an experimental setup, consisting of a dynamometer (FK 250, Fr. Sauter AG), a custom clamp and a custom sample holder fixed on a rail, was designed and built (see Fig. 4). The proper alignment of the whole test system was ensured by a positioning hole (alignment feature in Fig. 4b), designed on both the custom clamp and the samples. The adhesion tests were performed by slowly pulling the custom sample holder, which resulted in an increasing pulling force applied over the cement, until a rupture of the bonding occurred, and the steel sample completely detached from the concrete block.

Knowing the contact area of the sample, i.e., the treated surface area of the samples covered by the cement mixture, the shear strength σ was calculated as in Eq. (1), as the ratio between the maximum force F recorded by the dynamometer and the nominal contact area A_c [25]:

$$\sigma = \frac{F}{A_c} \tag{1}$$

For the untreated, LIPSS-treated and sandblasted samples, A_c was calculated as the product of the measured length L and width Q of the treated area (referring to Fig. 2 and Table 1). For laser-milled samples, the presence of a regular repetition of micro walls was taken into account, as shown in Eq. (2):

$$A_c = n{\cdot}A_i + m{\cdot}A_w \tag{2}$$

where A_i corresponds to the inner area of the n engraved channels and A_w to the surface area of the m micro-walls. A_i and A_w were computed using the following expressions, accounting for the geometric features of the texturing, as illustrated in Fig. 2 and Table 1:

$$A_i = 2(d{\cdot}L) + (w{\cdot}L) \tag{3}$$

$$A_W = b{\cdot}L \tag{4}$$

As previously mentioned, for each type of surface treatment/texture, four samples were tested to have a reliable average value of the shear strength (indicated in the following as average shear strength and expressed in MPa or N/cm^2).

3. Results and discussion

LIPSS structures have been induced on the stainless-steel samples by scanning the surface with an average power equal to 0.8 W and repetition rate of 50 kHz. Fig. 5 shows the ripples; as expected, these are linear and orthogonally oriented with respect to the polarization of the incident laser beam, characterized by a spatial periodicity of about 900 nm.

By using an average power equal to 5 W and a repetition rate of 50 kHz, rectangular channels with a depth of around 80 μm were ablated over the sample surface. In Fig. 6, it is possible to observe randomly distributed peaks and valleys on the bottom of the processed channels. Such pronounced features would act as potential additional interlocking sites where the cement can settle, adhere, and harden.

The surface roughness was evaluated via optical profilometry for untreated, sandblasted (two different duration of the sandblasting treatment), LIPSS-covered and laser textured samples. The results of such analysis are reported in Table 2; where in the case of textured samples, the channels' bottom roughness is reported. Exemplary three-dimensional profilometer images of the treated surfaces are shown in Fig. 7.

As mentioned before, for each kind of treatment (LIPSS, DLW, sandblasting for 20 s and 2 min) four samples were prepared according to the procedure explained in Section 2.2 and tested after thirty days as described in Section 2.3.2. After measuring the maximum pulling

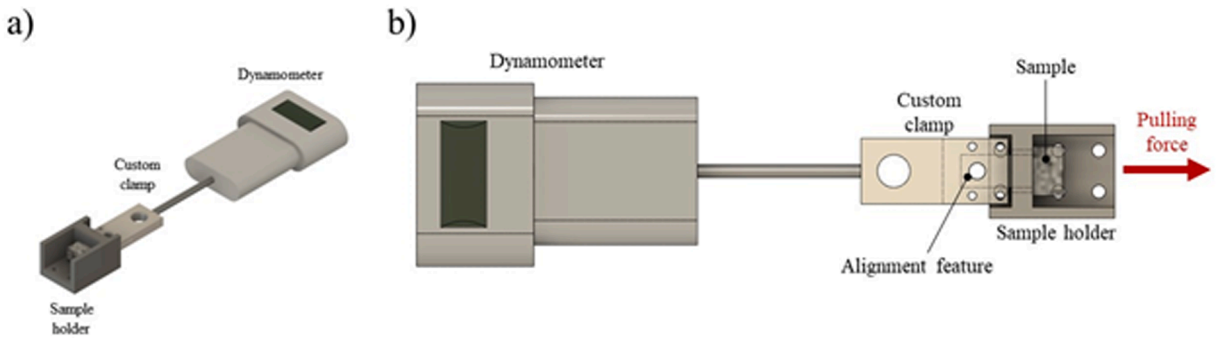

Fig. 4. (a) 3D render of the experimental setup for the adhesion texting with (b) sketch marking the direction of the force applied on the sample.

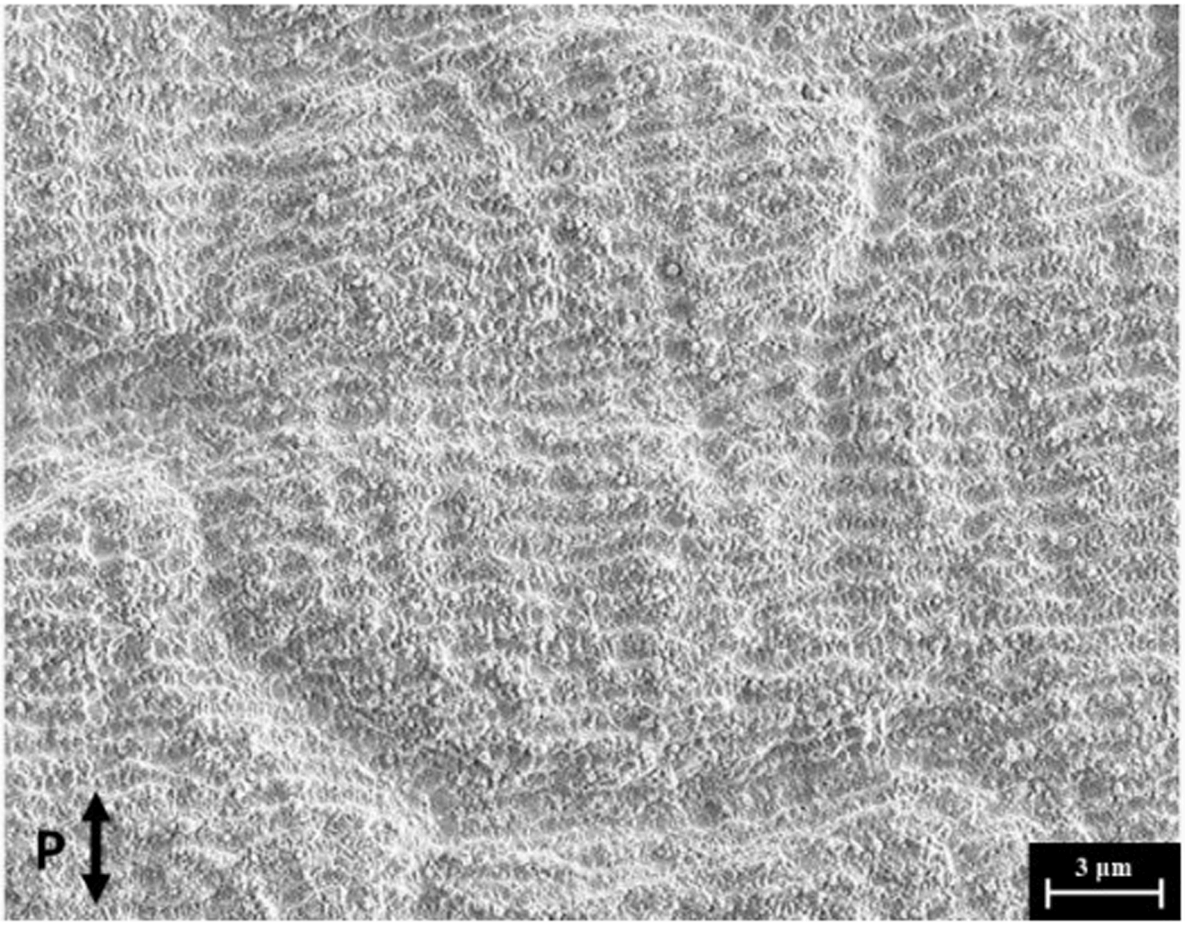

Fig. 5. SEM image of linear LIPSS induced over the sample, where the double arrow represents the polarization of the incident radiation.

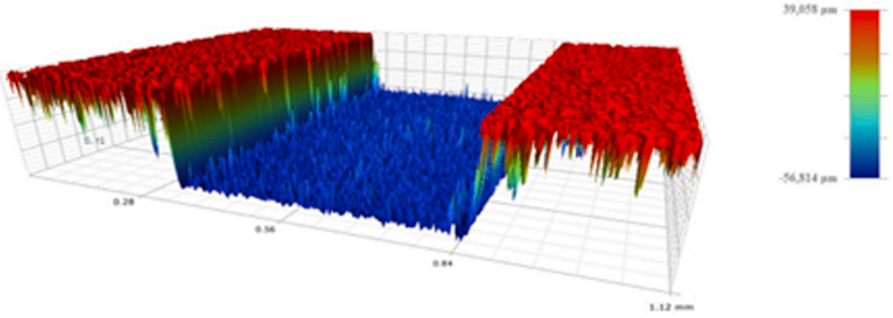

Fig. 6. 3D profile of a laser-milled channel obtained via optical profilometry.

strength before the detachment of the concrete block from the steel sample, the geometric contact area was determined for each sample, and the shear strength was estimated according to Eq. (1). For the untreated, LIPSS-treated and sandblasted sample, 400 mm^2 (20 × 20 mm^2) nominal contact area was considered. For the milled steel samples with longitudinal and transversal texture, the lateral surfaces of each channel were also included and computationally calculated, thus leading to a value of 511 mm^2. The results of the shear strengths averaged over the four samples for each kind of surface treatment are also reported in Table 2.

Fig. 8 illustrates a comparison between the values of the average shear strength obtained in all the experimental conditions.

From the results in Table 2, no significant difference in terms of surface roughness can be noticed between the untreated surfaces and the LIPSS-treated surfaces. Therefore, the apparent different shear strength obtained in the two cases (see Fig. 8 and Table 2) can be ascribed to a distinct chemical characteristic of the surface. Indeed, treatments with LIPSS led to a duplication in shear strength compared to the untextured and, therefore, to an increase of the adhesion between steel and concrete. This result is in agreement with what was reported by Makarova et al., where the interaction of laser nanostructured reinforcement bars with concrete was investigated, finding a straining force (from a standard pull-out test) almost double compared to untextured bars (from 226 N to 447 N) [22]. Rather than to the almost negligible increase of the surface roughness, this finding has to be ascribed to the super-hydrophilic behavior exhibited by the LIPSS-covered samples just after the laser treatment [26], which is believed to enhance the spread and the adhesion of the water-based cement mixture over the surface.

On the other hand, in Fig. 7 and Table 2, it can be observed that the

Table 2
Surface roughness data for untreated, sandblasted and LIPSS-covered samples and average shear strength values obtained with all the treatments. As a comparison, in the case of textured samples, the texture characteristics shown in Table 1 will be considered rather than the roughness.

Surface treatment	Average roughness S_a (μm)	Root mean square average S_q (μm)	Average shear strength (N/cm^2) after 30 days
Untreated	0.31 ± 0.03	0.41 ± 0.04	1.9 ± 0.1
LIPSS treatment	0.34 ± 0.03	0.43 ± 0.04	3.1 ± 0.5
Sandblasted (20 s)	0.42 ± 0.08	0.61 ± 0.06	4.2 ± 1.3
Sandblasted (2 min)	2.50 ± 0.50	3.7 ± 0.4	7.1 ± 5.6
Longitudinal texture	1.65 ± 0.16	2.1 ± 0.2	8.1 ± 2.5
Transversal texture			30.6 ± 8.1

longer the exposure time to sandblasting, the more pronounced are the surface asperities. In this case, the average shear strength values seem to be strongly correlated to the surface roughness of the sample. In fact, a two-minutes sandblasting treatment led to a four-fold shear strength compared to the untreated sample, while twenty seconds-long treatment led only to a 2-fold increase, demonstrating the significant dependence of the adhesion behavior on the surface roughness. This results is in good agreement with [19] where the authors generated random roughness by laser surface texturing, showing a noticeable increase of the adhesion of TiAlN and AlCrN coatings to cemented carbide inserts. The main reason for this behavior can be attributed to the mechanical anchoring occurring within the surface features, in good agreement with [13,19].

In the case of DLW processed samples, in Fig. 8 and Table 2 are reported the testing results, showing an important increase in adhesion in terms of shear strength. In the longitudinal case a four-fold increase was observed compared to the untreated sample. A similar increasing trend of the adhesion was reported in [20]. In this case, an increase of the adhesion of SW-2 adhesive on 30CrMnSiA around 219% was found by performing a groove patterned surfaces. Moreover, as suggested in [21], orienting the texture perpendicularly to the load direction may enhance the final adhesive strength. This is what it was found with the transverse texture shown in Fig. 2, where a remarkable sixteen-fold increase in shear strength was noticed.

Such significative enhancement of adhesion can be attributed to the mechanical anchoring induced by the surface topography of the samples; the DLW milled channels become anchor points for the mixture, promoting mechanical interlocking with the treated surface. Furthermore, the additional enhanced surface roughness within the channel due to laser ablation even further promotes the mechanical anchoring (see Fig. 6) [18].

In addition, as schematically represented in Fig. 9, when transversal texturing was employed, the direction of the force applied during the pull-out tests is perpendicular to the direction of the engraved channels, thus creating a contrasting effect and providing a higher mechanical resistance against it. We ascribed the highest force recorded by the system in this case as due also to this effect. Conversely, in the case of longitudinal texture, the contribution of the aforementioned mechanism is lower due to the fact that the force does not oppose the interlocking design as the transversal one, therefore the contribution is much smaller. The obtained result highlights the importance of a well-designed texture, proving to be an essential step to substantially enhance the adhesion between steel and concrete.

Once the adhesion tests of the samples were performed, EDX was employed to identify the presence of residual cement on the steel samples, especially inside the laser milled channels. To this aim, the percentage of Ca, as one of the main chemical elements constituting the

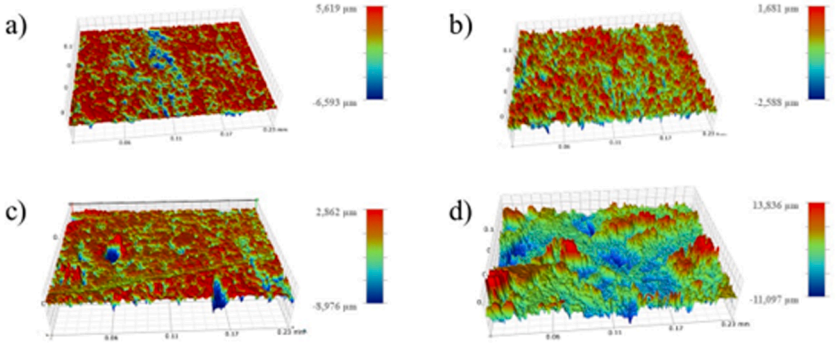

Fig. 7. 3D surfaces obtained via optical profilometry of (a) untreated surface, (b) LIPSS-treated surface, (c) 20 s sandblasted surface and (d) 2 min sandblasted surface.

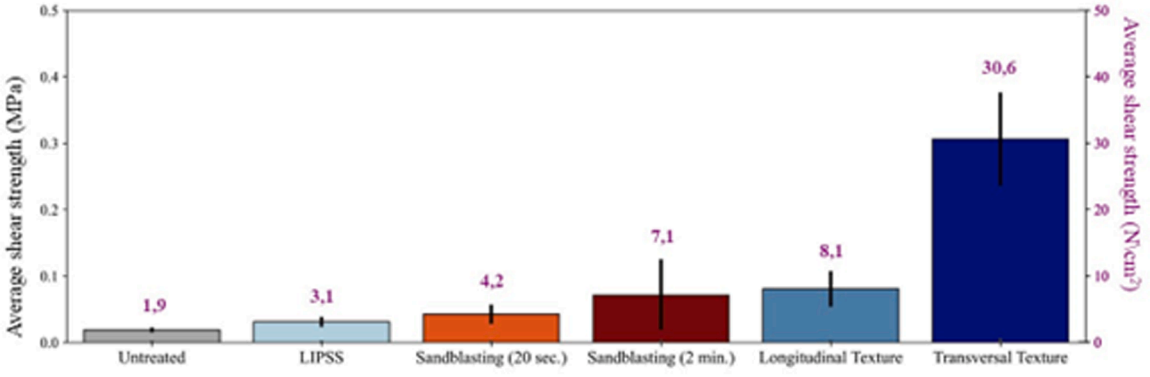

Fig. 8. Comparison of the average shear strength for the different surface treatments after 30 days.

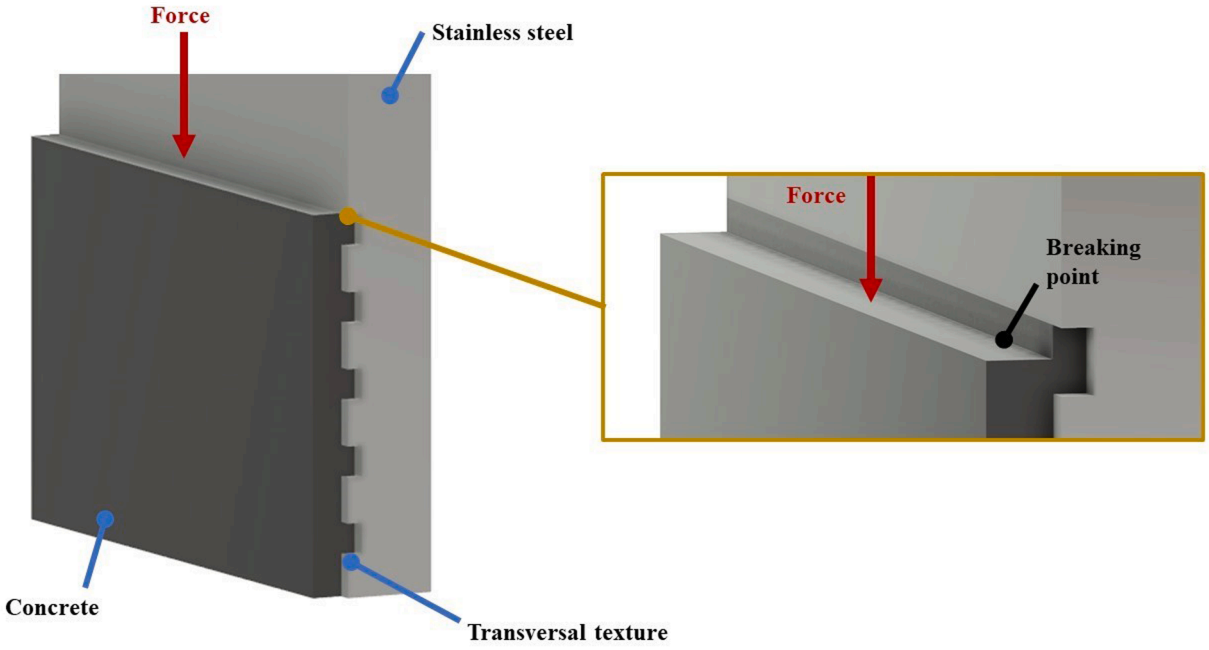

Fig. 9. Graphical representation of the mechanical contrast of the cement mixture inside the channel during an experimental test, causing the break of it, so representing an optimal texture to counteract the applied force.

cement [27], was evaluated. A comparison of Ca percentage measured in areas inside the engraved channels and areas on the untextured parts of the steel target is presented in Fig. 10, along with the associated weight percentages of other detected species and the related uncertainties.

Lastly, the EDX spectra of the transversal textured sample show a more pronounced calcium presence inside the engraved channel with respect to the untreated area, representing a weight percentage of 10%. This higher concentration of calcium within the channel suggests an improved mechanical interlocking adhesion between the cement and the steel surface, potentially reinforced by the increased roughness of the bottom of the channel due to the laser ablation process. The results obtained from this analysis suggest that the geometric features of the texture promote its filling, as the presence of calcium signifies its occupation.

4. Conclusions

The aim of this study was to investigate the effect of different treatments to modify the surface topography of steel targets to improve their adhesion with a concrete mixture, by promoting the formation of interlocking sites. To this aim two laser texturing techniques, i.e., Direct Laser Writing (DLW) and the generation of Laser Induced Surface Structures (LIPSS), were employed and compared to the conventional abrasive technique of sandblasting.

Though LIPSS did not significantly modified the surface roughness of the treated samples (only 10% increase of Sa was found), such treatment resulted in about 2-fold higher average shear strength. This is believed to be due to the superhydrophilicity of the freshly treated samples [20], which helps in spreading the water-based cement mixture, thus contributing to the improvement of its adhesion onto the LIPSS covered samples.

However, it is well known that the surface roughness plays a central role on the adhesion mechanism [24]. This was also confirmed in this work, where a slight increase of the surface roughness (Sa= 0.34 μm, compared to the untextured samples roughness of 0.31 μm), obtained by a 20 s-long sandblasting, resulted in a 2-fold higher average shear stress. A much rougher surface was obtained, instead, by a 2 min-long sandblasting (Sa = 2.50 μm), which resulted in about 4 times higher average shear strength.

The best results in terms of adhesion enhancement were obtained

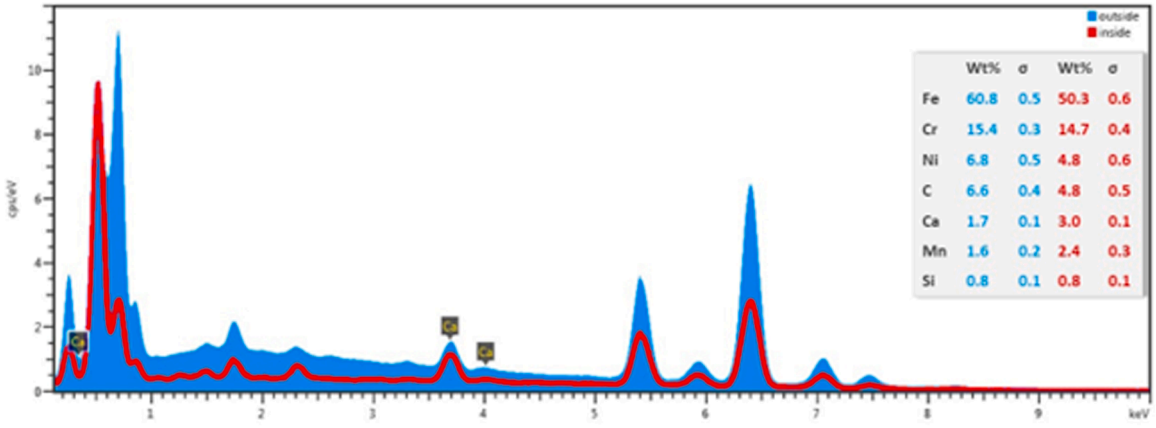

Fig. 10. EDX spectrum of the inside of one channel and the outer part region of the transversal sample.

with samples where regular repetitions of micro-channels and micro-walls were generated on their surface by Direct Laser Writing. Two different textures arrangements were tested, i.e., longitudinal, and transversal micro-channels, which resulted in about 4 times and 16 times higher average shear strength, respectively, compared to the untextured case EDX analysis confirmed that these surface morphologies were able to trap cement particles and oppose to the detachment of cured concrete when pull-out tests were performed. The better effectiveness of transversal textured samples can be ascribed to the arrangement of the textures features which, being perpendicular to the applied force, contrasts it, and thus cause a much higher pull-out stress to be required to reach the detachment. This suggests that when designing the surface texture of a metallic specimen to be treated to increase its adhesion to cement, it is important to focus on the direction of stresses it is typically subjected to, in order to define the topography that better contrasts the tendency to the detachment due to the external forces. Laser technology, thanks to its high degree of precision and flexibility, is the best option to meet such requirements and to easily reconfigure the designs for each proof-of concept application.

CRediT authorship contribution statement

Marida Pontrandolfi: Formal analysis, Data curation, Conceptualization, Investigation, Methodology, Resources, Validation, Visualization, Writing – original draft, Writing – review & editing. **Caterina Gaudiuso:** Conceptualization, Funding acquisition, Methodology, Supervision, Writing – review & editing. **Francesco Paolo Mezzapesa:** Funding acquisition, Writing – review & editing. **Annalisa Volpe:** Writing – review & editing. **Myriam Bevillon:** Writing – review & editing, Funding acquisition. **Antonio Ancona:** Writing – review & editing, Supervision, Project administration, Funding acquisition.

Declaration of competing interest

The authors declare that they have no known competing financial interests or personal relationships that could have appeared to influence the work reported in this paper.

Data availability

Data will be made available on request.

Acknowledgements

The financial support to this work by the Apulian Region within the framework of the Gunnebo Innovation Hub project and by the European Union - *Next Generation* EU within the project ELATED - Enhanced LAser spectroscopy TEchniques for autism Diagnosis in children (grant number: P2022YTFHY) are gratefully acknowledged. Pietro Paolo Calabrese is kindly acknowledged for his technical support.

References

[1] H. Jiang e M. G. Chorzepa, «Aircraft impact analysis of nuclear safety-related concrete structures: a review», Eng. Fail Anal. 46 (2014) 118–133, https://doi.org/10.1016/j.engfailanal.2014.08.008.

[2] A. Baričević, M. Jelčić Rukavina, M. Pezer, N e, Štirmer, «Influence of recycled tire polymer fibers on concrete properties», Cem. Concr. Compos. 91 (2018) 29–41, https://doi.org/10.1016/j.cemconcomp.2018.04.009.

[3] J.-M. Yang, H.-O. Shin, D.-Y. Yoo, «Benefits of using amorphous metallic fibers in concrete pavement for long-term performance», Arch. Civil Mech. Eng. 17 (4) (2017) 750–760, https://doi.org/10.1016/j.acme.2017.02.010.

[4] M.S. Ahamed, P. Ravichandran, A.R. Krishnaraja, «Natural fibers in concrete – a review», IOP Conf. Ser.: Mater. Sci. Eng. 1055 (1) (2021) https://doi.org/10.1088/1757-899X/1055/1/012038.

[5] G.S. Duffó, W. Morris, I. Raspini, C. Saragovi, «A study of steel rebars embedded in concrete during 65 years», Corros. Sci. 46 (9) (2004) 2143–2157, https://doi.org/10.1016/j.corsci.2004.01.006.

[6] A.B. Kizilkanat, N. Kabay, V. Akyüncü, S. Chowdhury, A.H. Akça, «Mechanical properties and fracture behavior of basalt and glass fiber reinforced concrete: an experimental study», Constr. Build. Mater. 100 (2015) 218–224, https://doi.org/10.1016/j.conbuildmat.2015.10.006.

[7] J. Thomas, A. Ramaswamy, «Mechanical properties of steel fiber-reinforced concrete», J. Mater. Civil Eng. 19 (5) (2007) 385–392, https://doi.org/10.1061/(ASCE)0899-1561(2007)19:5(385).

[8] D. Benarbia, M. Benguediab, «Propagation of cracks in reinforced concrete beams cracked and repaired by composite materials», Mech. Mech. Eng. 21 (3) (2017).

[9] X. Fu, D.D.L. Chung, «Improving the bond strength between steel rebar and concrete by ozone treatment of rebar and polymer addition to concrete», Cem. Concr. Res. 27 (5) (1997) https://doi.org/10.1016/S0008-8846(97)00057-4.

[10] X. Fu, D.D.L. Chung, «Combined use of silica fume and methylcellulose as admixtures in concrete for increasing the bond strength between concrete and steel rebar 11Communicated by D.M. Roy.», Cem. Concr. Res. 28 (4) (1998) 487–492, https://doi.org/10.1016/S0008-8846(98)00016-7.

[11] L. Libessart, P. de Caro, C. Djelal, I. Dubois, «Correlation between adhesion energy of release agents on the formwork and demoulding performances», Constr. Build. Mater. 76 (2015) 130–139, https://doi.org/10.1016/j.conbuildmat.2014.11.061.

[12] N. Coniglio, N. Spitz, M.El Mansori, «Designing metallic surfaces in contact with hardening fresh concrete: a review», Constr. Build. Mater. 255 (2020) 119384 https://doi.org/10.1016/j.conbuildmat.2020.119384.

[13] J. Hou, X. Fu, D.D.L. Chung, «Improving both bond strength and corrosion resistance of steel rebar in concrete by water immersion or sand blasting of rebar», Cem. Concr. Res. 27 (5) (1997) 679–684, https://doi.org/10.1016/S0008-8846(97)00043-4.

[14] C. Putignano, G. Parente, F.J. Profito, C. Gaudiuso, A. Ancona, G. Carbone, «Laser microtextured surfaces for friction reduction: does the pattern matter?», Materials (Basel) 13 (2020) https://doi.org/10.3390/ma13214915.

[15] S. Yan, et al., «Fabrication and tribological characterization of laser textured engineering ceramics: si3N4, SiC and ZrO2», Ceram. Int. 47 (10, Part A) (2021) 13789–13805, https://doi.org/10.1016/j.ceramint.2021.01.244.

[16] C. Gaudiuso, F. Fanelli, F.P. Mezzapesa, A. Volpe, A. Ancona, «Tailoring the wettability of surface-textured copper using sub-THz bursts of femtosecond laser pulses», Appl. Surf. Sci. 638 (2023) 158032 https://doi.org/10.1016/j.apsusc.2023.158032.

[17] D. Meena Narayana Menon, M. Giardino, D. Janner, «Tunable pulsewidth nanosecond laser texturing: from environment friendly superhydrophobic to superamphiphobic surfaces», Appl. Surf. Sci. 610 (2023) 155356 https://doi.org/10.1016/j.apsusc.2022.155356.

[18] N. Naat, Y. Boutar, S. Naïmi, S. Mezlini, L.F.M. Da Silva, «Effect of surface texture on the mechanical performance of bonded joints: a review», J. Adhes. 99 (2) (2023) 166–258, https://doi.org/10.1080/00218464.2021.2008370.

[19] R. Viana, M.S.F. de Lima, W.F. Sales, W.M. da Silva Jr., Á.R. Machado, «Laser texturing of substrate of coated tools — performance during machining and in adhesion tests», Surf. Coati. Technol. 276 (2015) 485–501, https://doi.org/10.1016/j.surfcoat.2015.06.025.

[20] Z. Feng, et al., «Effect of laser texturing on the surface characteristics and bonding property of 30CrMnSiA steel adhesive joints», J. Manuf. Process. 47 (2019) 219–228, https://doi.org/10.1016/j.jmapro.2019.09.046.

[21] L. Guo, J. Liu, H. Xia, X. Li, X. Zhang, H. Yang, «Effects of surface treatment and adhesive thickness on the shear strength of precision bonded joints», Polym. Test. 94 (2021) 107063 https://doi.org/10.1016/j.polymertesting.2021.107063.

[22] N.V. Makarova, S.V. Makarov, «Femtosecond laser nanostructuring of reinforcement bars surface for improvement of its interaction with concrete», in: Journal of Physics: Conference Series, IOP Publishing, 2018 012082.

[23] F.M.C. Capodacqua, A. Volpe, C. Gaudiuso, A. Ancona, «Bonding of PMMA to silicon by femtosecond laser pulses», Sci. Rep. 13 (2023) https://doi.org/10.1038/s41598-023-31969-y.

[24] S.K. Roy Chowdhury, H.M. Pollock, «Adhesion between metal surfaces: the effect of surface roughness», Wear. 66 (3) (1981) 307–321, https://doi.org/10.1016/0043-1648(81)90124-1.

[25] A. Hamilton, Y. Xu, M.E. Kartal, N. Gadegaard, D.M. Mulvihill, «Enhancing strength and toughness of adhesive joints via micro-structured mechanical interlocking», Int. J. Adhes. Adhesives 105 (2021) 102775 https://doi.org/10.1016/j.ijadhadh.2020.102775.

[26] G. Giannuzzi, et al., «Short and long term surface chemistry and wetting behaviour of stainless steel with 1D and 2D periodic structures induced by bursts of femtosecond laser pulses», Appl. Surf. Sci. 494 (2019) 1055–1065, https://doi.org/10.1016/j.apsusc.2019.07.126.

[27] D.D. Double, A. Hellawell, S.J. Perry, P.B. Hirsch, «The hydration of Portland cement», Proc. R. Soc. Lond. A. Math. Phys. Sci. 359 (1699) (1997) 435–451, https://doi.org/10.1098/rspa.1978.0050.